Taylor & Francis
Taylor & Francis Group

RESEARCH ARTICLE

🔓 OPEN ACCESS   🅜 Check for updates

Hepatoprotective effect and metabonomics studies of radix gentianae in rats with acute liver injury

Shizhao Xu, Fanli Kong, Zhengwu Sun, Yalin Xi, Fei Qi and Jianzhi Sun

Dalian Municipal Central Hospital Affiliated of Dalian Medical University, Dalian, China

ABSTRACT

Context: As a well-known traditional Chinese medicine for protecting the liver, the mechanism of Radix Gentianae (RG) remains unclear.

Objective: The hepatoprotective effect and metabonomics of RG were studied to explore the molecular and metabolic mechanisms of RG protecting the liver.

Materials and methods: Sprague-Dawley rats were divided into control and model group ($n = 10$, orally given distilled water), intervention group (4 subgroups, $n = 10$, prophylactically and orally given 0.63, 2.5 and 5.6 g/kg RG and 0.2 g/kg bifendatatum for 7 d). On day 7 of the intervention, all rats except the control were injected intraperitoneally with 2.5% carbon tetrachloride vegetable oil solution (1.5 mL/kg) to induce liver injury. After 24 h of carbon tetrachloride injection, rat serum and liver tissue were collected for determining AST, ALT, TNF-α, MCP-1, IL-6, SOD, MDA, GSH, and GSH-PX. Rat serum was used for analysing endogenous metabolism by UPLC-Q-TOF-MS.

Results: Different doses of RG can significantly decrease the levels of AST, ALT, TNF-α, MCP-1, IL-6 and MDA, and increase the levels of SOD, GSH, and GSH-PX in rats with liver injury ($p < 0.05$; TNF-α, and IL-6, $p < 0.05$ only at 5.6 g/kg dose). Eight biomarkers of liver injury were obtained in serum metabonomics, involving five significant metabolic pathways. RG can improve steroid biosynthesis, linoleic acid metabolism, porphyrin and chlorophyll metabolism, and fatty acid biosynthesis.

Conclusion: RG demonstrated a good ability to protect the liver and improving endogenous metabolism in rats with liver injury. This can help us understand the mechanism of RG and more clinical verifications were inspired.

Introduction

The liver is the largest substantial organ in the human body, it performs many functions including synthesis, catabolism, biotransformation, and internal and external secretion of substances. The liver blood supply is rich and easily attacked by various pathogenic factors and stimulating factors *in vitro* and *in vivo*, causing the inflammatory response of the liver, leading to liver injury (Luan and Ju 2018). As a common clinical disease, liver injury has always been one of the key research objects in medicine and pharmacy (Okubo et al. 2016; Zeeshan et al. 2019).

Radix Gentianae (RG), a well-known traditional Chinese medicine (TCM), is the dry roots and rhizomes of *Gentiana manshurica* Kitag. (Gentianaceae), *Gentiana scabra* Bge. (Gentianaceae), *Gentiana triflora* Pall. (Gentianaceae), or *Gentiana rigescens* Franch. (Gentianaceae) and has the effect of clearing away heat, drying dampness, protecting the liver, and benefiting the gallbladder (Chinese Pharmacopoeia Commission 2015). RG was first recorded in Shennong herbal classic. It has been used to protect the liver for many years in China. In the clinical practice of TCM, some TCM compounds consisting of RG, such as Longdanxiegan decoction, Xieqing pill and Dangguilonghui pill, are often used to treat liver diseases (Ren et al. 2019; Chen et al. 2018).

The existing clinical effects and experimental studies showed that RG played an excellent role in protecting the liver (Qu et al. 2015; Zhang et al. 2019). Previous studies have shown that the mechanism of RG protecting the liver is related to alleviating oxidative stress and reducing inflammatory expression *in vivo* (Xia et al. 2017; Ding 2020). However, we still have a limited understanding of the mechanism of its efficacy. In particular, the characteristics of multi-component and multi-target of TCM make it difficult for us to study and understand the mechanism. The action of TCM on the human body is a complex biological process, and its effect will be reflected in the corresponding gene, protein, and metabonomics level (Plumb et al. 2006). Metabonomics, as a subject developed after genomics and proteomics, can comprehensively monitor the changes of metabolites in the body, which is more in line with the characteristics of multi-component, multi-target and integrated regulation of TCM, and the holistic, dynamic and dialectical views of TCM theory (Yang et al. 2019). Metabonomics technology is also widely used in the study of the mechanism of action of TCM (Wu et al. 2020; Zhang et al. 2020).

In this study, we injected carbon tetrachloride into the abdominal cavity of rats to duplicate the model of acute liver injury and evaluated the protective effect of RG on the liver at the molecular level. On this basis, metabonomics was used to study the changes of endogenous metabolites in serum after the

CONTACT Shizhao Xu ✉ dazhao666@163.com 🏥 Dalian Municipal Central Hospital Affiliated Of Dalian Medical University, Dalian, China

intervention of RG, to reveal the mechanism of RG against liver injury from the overall metabolic pathway.

Materials and methods

Medicinal materials

RG was purchased from the planting base of Qingyuan (Liaoning, China) in May 2018, identified as the dried rhizome of *Gentiana scabra* by Professor Feng Li (Liaoning University of TCM, Dalian, China). The voucher specimen (number: 20180716004) was deposited in the Herbarium of Liaoning University of TCM (Dalian, China). RG powder (50 g) was soaked in 500 mL water for 0.5 h, heated and decocted for 1 h, filtered while hot, then an additional 400 mL water was added to be decocted again for 1 h, filtered while hot and the two filtrates were combined, and concentrated to 90 mL to obtain 0.56 g/mL solution. 0.56 g/mL solution (30 mL) was diluted to 67 mL with water to obtain 0.25 g/mL solution. 0.56 g/mL solution (10 mL) was diluted to 87 mL with water to obtain 0.063 g/mL solution. 0.063, 0.25, 0.56 g/mL were regarded as low, medium, and high dosage solutions of RG, respectively.

Bifendatatum drop pills (batch number: h33021305) were purchased from Zhejiang Wanbang Pharmaceutical Co., Ltd. (Zhejiang, China). Bifendatatum drop pills (600 mg) were powdered and dissolved in 30 mL distilled water to a 20 mg/mL Bifendatatum solution as a positive control drug.

Reagents

Carbon tetrachloride (batch number: 160922) was purchased from Shenyang reagent No.5 factory (Liaoning, China). Aspartate aminotransferase (AST), alanine aminotransferase (ALT), tumour necrosis factor-α (TNF-α), monocyte chemoattractant protein-1 (MCP-1), interleukin-6 (IL-6), superoxide dismutase (SOD), malondialdehyde (MDA), glutathione (GSH), glutathione peroxidase (GSH-PX) quantitative kits (batch number: 201709) were purchased from Shanghai Kexing Trading Co., Ltd. (Shanghai, China).

Animals and groups

Specific pathogen-free male Sprague-Dawley rats (200 ± 20 g) were purchased from Liaoning Changsheng Biotechnology Co., Ltd. (license number: SCXK(Liao)2010-0001, Liaoning, China) and randomly divided into six groups ($n = 10$): (1) the control (CG); (2) the model (MG); (3) the Bifendatatum positive control (PCG); (4) the low dose of RG (LRGG); (5) the medium group of RG (MRGG); (6) the high dose of RG (HRGG). The rats in each administration group were given corresponding solution (10 mL/kg) by regular gavage every day for 7 d, and the rats in the control group and the model group were given distilled water by gavage. One hour after the last administration, a 2.5% carbon tetrachloride vegetable oil solution was injected intraperitoneally at a dose of 1.5 mL/kg to replicate the acute liver injury model. This animal study was approved by the Ethics Committee of Dalian Central Hospital, Dalian, China (approval number: 2017-010-22).

Sample collection

All rats were anaesthetised by intraperitoneal injection of chloral hydrate (30 mg/kg) after fasting for 24 h. Abdominal aorta blood samples were collected and centrifuged for 10 min (4000 rpm, 4 °C). Serum was separated and stored at −80 °C until analysis. The liver tissue was collected, washed with normal saline, weighed, and put into 10 mL centrifuge tube. The liver tissue was added hypothermic saline and homogenised, the supernatant was obtained after centrifugation for 10 min (12,000 rpm, 4 °C).

Pathological sections of liver tissue

A small piece of liver tissue at the same location of rats from different groups was collected, fixed with 10% formaldehyde, then dehydrated, made transparent, soaked with wax, embedded, sliced, dewaxed, stained with hematoxylin-eosin, dehydrated and made transparent, and sealed successively. Pathological sections of liver tissue were observed and photographed under a microscope (×200).

Biochemical analysis

The levels of AST, ALT, TNF-α, MCP-1, IL-6 in serum and SOD, MDA, GSH, GSH-PX in liver tissue in rats of each group were detected by enzyme-linked immunosorbent assay (ELISA). The operation was carried out in strict accordance with the kit's instructions.

Pre-treatment of metabonomics samples

The serum samples from the CG group, the MG group, and the MRGG group were chosen for the metabonomics study. A serum sample (200 μL) was taken, 600 μL methanol was added and mixed to precipitate the protein. All supernatant was absorbed and transferred after centrifugation for 10 min (12,000 rpm, 4 °C). The supernatant was dried by nitrogen airflow, then redissolved by adding 100 μL methanol and vortexed for 2 min. The supernatant (100 μL) was obtained after centrifugation for 10 min (12,000 rpm, 4 °C) and filtered by a 0.22 μm filter membrane for ultra-performance liquid chromatography coupled with a quadrupole time-of-flight mass spectrometry (UPLC-Q-TOF-MS) injection analysis. Each sample (20 μL) was taken equally and mixed as a quality control (QC) sample. QC sample was injected every 10 samples intervals to test the stability and repeatability of the instrument.

Chromatography and mass spectrometry conditions

Chromatographic experiments were performed on a Waters Acquity UPLC HSS T3 column (2.1 × 100 mm, 1.8 μm) using an Acquity UPLC™ System (Waters Corp., Milford, MA, USA). The column temperature was set at 40 °C with an injection volume of 5 μL, and the mobile phase consisted of solvent A (0.1% formic acid in water) and solvent B (0.1% formic acid in acetonitrile) at a flow rate of 0.3 mL/min. The gradient elution procedure was as follows: 0–5 min, 35–50% B; 5–10 min, 50–78% B; 10–15 min, 78–80% B; 15–18 min, 80–35% B; 18–20 min, 35–35% B.

Mass spectrometry was performed on a Xevo G2-XS Q-TOF/MS (Waters Corp., Milford, CT, USA). The instrument was operated by using an electrospray ion (ESI) source in positive

and negative mode. The ionisation source conditions were as follows: capillary voltage, 2.0 kV; source temperature, 100 °C; dissolvent gas temperature, 400 °C; cone voltage, 40 V. Nitrogen was used as desolvation and cone gas with a flow rate of 800 and 100 L/h, respectively. MS^E scanning mode was used to detect, leucine-enkephalin was used as the correction solution, and lock mass function was used to calibrate the collected data in real-time. The collision energy of the low energy channel was 2 V, the collision energy of the high energy channel was 20–30 V, and the mass scanning range was 100–1200 m/z.

Strategy for analysis of metabonomics

Masslynx 4.1 software (Waters, USA) was used to analyse the raw data, the normalised label-free results of the metabolic peaks of each sample were obtained. The normalisation across samples was based on the total ionic strength of each chromatogram. The data matrix composed of sample code, RT-m/z pair, and peak area was imported into Simca-p 14.0 software for principal component analysis (PCA) and orthogonal partial least squares discriminant analysis (OPLS-DA). According to the results of OPLS-DA analysis of the control and model groups, variable importance in projection (VIP) list files were created, and metabolic variables with VIP value > 1 and $p < 0.05$ of independent-samples t-test were obtained for further analysis. Combined with the public database such as HMDB (http://www.hmdb.ca/), KEGG (http://www.genome.jp/kegg/), METLIN (https://metlin.scripps.edu) and related literature, the structure of potential biomarkers of liver injury was identified. The name of the identified biomarker was imported into metabo analyst 4.0 website (http://www.metaboanalyst.ca/) to analyse and determine the disturbed metabolic pathway. According to the standard of impact > 0, the metabolic pathway closely related to liver injury was obtained. On this basis, the regulatory effect of RG on biomarkers and main metabolic pathways was observed to speculate the recovery effect of RG on body function under liver injury.

Statistical analysis

All results were displayed as Mean ± Standard Deviation. Statistical analysis was carried out using SPSS 17.0 software. Differences were assessed by one-way ANOVA with Bonferroni method, and there was a statistically significant difference between the two groups when p-value < 0.05.

Results

### Pathological sections of liver tissue

The pathological sections of liver tissue of rats in each group were shown in Figure 1. In the CG group, the hepatocytes were arranged orderly in a cord shape, the space between hepatic sinusoid was moderate, the size of hepatocytes was normal, and there were no inflammatory cells infiltration and abnormal morphological structure changes. In the MG group, the liver tissue was stained unevenly, the size of hepatocytes was not equal, there were vacuoles, the boundary of cells was not clear, the arrangement of hepatocytes was irregular, the hepatic sinusoid was fuzzy, congestion and inflammatory cells infiltration can be observed, and there were necrotic hepatocytes. In the PCG group, the morphological structure of the liver tissue was improved, the vacuoles basically disappeared, the size of the hepatocytes changed, and the boundary was basically clear. Similarly, the recovery of hepatocytes can be clearly observed in different degrees in different doses of the RG administration group, and the recovery effect of MRGG and HRGG groups was better than that of the LRGG group.

Biochemical analysis

As was shown in Figure 2, compared with the CG group, the contents of AST, ALT, TNF-α, MCP-1, IL-6, and MDA in the MG group significantly increased ($p < 0.05$) while the contents of
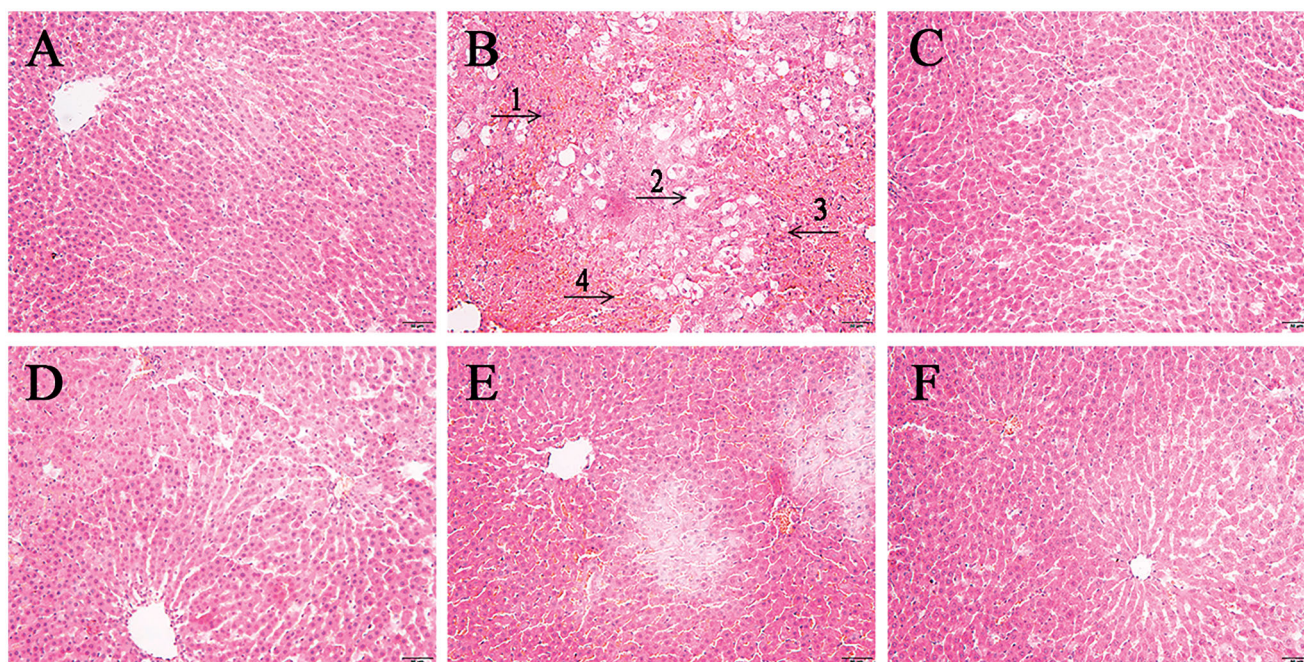
Figure 1. The pathological sections of liver tissue of rats among diverse groups (×200): (A) the control group (CG); (B) the model group (MG); (C) the Bifendatatum positive control group (PCG); (D) the low dose group of RG (LRGG); (E) the medium-dose group of RG (MRGG); (F) the high dose group of RG (HRGG). (1. The size and morphology of hepatocytes were abnormal; 2. There were lots of vacuoles; 3. The shape of the liver cord was changed; 4. The hepatic sinusoid was fuzzy).
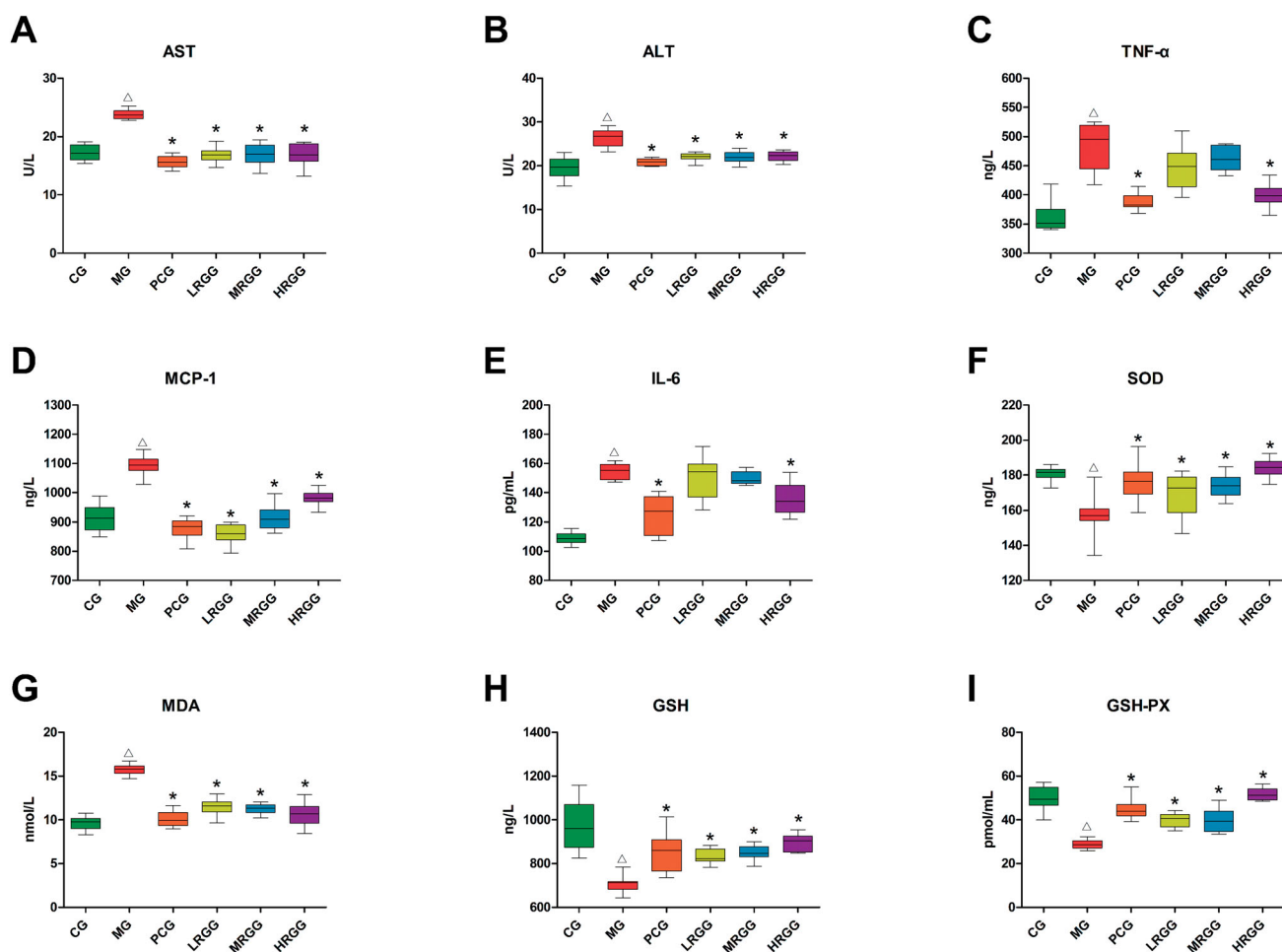
Figure 2. The contents of biochemical indexes in serum and liver of rats among diverse groups ($n = 10$): (A) Aspartate aminotransferase (AST) level; (B) alanine amino-transferase (ALT) level; (C) tumour necrosis factor-α (TNF-α) level; (D) monocyte chemoattractant protein-1 (MCP-1) level; (E) interleukin-6 (IL-6) level; (F) superoxide dismutase (SOD) level; (G) malondialdehyde (MDA) level; (H) glutathione (GSH) level; (I) glutathione peroxidase (GSH-PX) level. $^{\triangle}p < 0.05$ when compared with the CG group; $^{*}p < 0.05$ when compared with the MG group.

SOD, GSH, and GSH-PX significantly decreased ($p < 0.05$). Compared with the MG group, the contents of AST, ALT, TNF-α, MCP-1, IL-6, and MDA in the PCG group significantly decreased ($p < 0.05$) while the contents of SOD, GSH, and GSH-PX significantly increased ($p < 0.05$). The contents of AST, ALT, MCP-1, and MDA in the LRGG and MRGG group significantly decreased ($p < 0.05$) while the contents of SOD, GSH, and GSH-PX significantly increased ($p < 0.05$). The contents of AST, ALT, TNF-α, MCP-1, and MDA in the HRGG group significantly decreased ($p < 0.05$) while the contents of SOD, GSH, and GSH-PX significantly increased ($p < 0.05$).

## Metabonomics analysis

Metabonomics method validation

The relative standard deviation (RSD) of all peaks in QC samples was <30% by calculation. The PCA scores (Figure 3) showed that the plots of QC samples were well gathered under positive and negative ions, and close to the centre of the circle. These showed that the repeatability of the detection results was good and the instrument was stable, and it is suitable for the metabonomics analysis of batch samples.

PCA analysis

The PCA scores (Figure 3) showed that each group was independently gathered in a pile under the positive and negative ion mode, representing a relatively stable instrument detection ability. The CG group and MG group were separated completely, indicating that there were differences in metabolic profiles between the two groups and verifying the successful replication of the animal model of liver injury. The Radix Gentianae group (RGG) lay between the CG and MG groups and had a tendency to move from the MG group to the CG group, suggesting that the RGG group had a recovery trend from liver injury. The model parameters R^2X and Q^2 of PCA were relatively close to 1, indicating that the PCA model was reliable.

OPLS-DA analysis

The OPLS-DA scores of CG vs. MG (Figure 4A1, B1) showed that the CG group and MG group were separated completely under the positive and negative ion mode, indicating that the metabolism in rats with liver injury had obvious changes compared with the healthy rats. The OPLS-DA scores of all groups (Figure 4A2, B2) showed that the CG group and MG group were separated completely under the positive and negative ion mode, and the RGG lay between the CG and MG groups, indicating
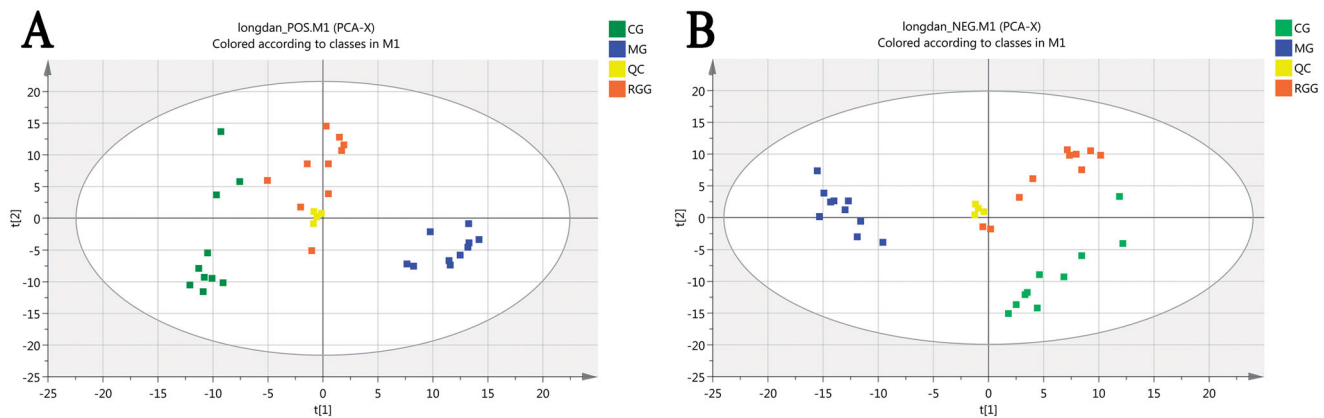
Figure 3. The scores of principal component analysis: (A) Positive ion mode; (B) Negative ion mode (model parameters-A: $R^2X = 0.696$, $Q^2 = 0.525$; B: $R^2X = 0.724$, $Q^2 = 0.643$).

that the metabolism of rats with liver injury tended to be improved to normal state after the intervention of RG. The model parameters R^2Y and Q^2 of OPLS-DA were relatively close to 1, indicating that the OPLS-DA model was reliable. The results of 200 times permutation tests of the OPLS-DA model were also shown in Figure 4, R^2 and Q^2 values generated by any random permutation on the left were all less than the original values on the right, proving that the prediction ability of the model was greater than that of any random permutation of Y variables, indicating that each OPLS-DA model was not over fitted and the OPLS-DA results were accurate.

Identification of the potential biomarkers of liver injury

As was shown in Table 1, eight potential biomarkers were putatively identified under positive and negative mode. The identification error of all metabolites was within 5 ppm. Compared with the CG group, the levels of cholic acid, arachidonic acid, and chenodeoxycholic acid in the MG group significantly increased, while the levels of lathosterol, oleic acid, bilirubin, linoleic acid, and palmitic acid significantly decreased.

Metabolic pathway analysis

The result of metabolic pathway analysis was shown in Figure 5, each circle represented a metabolic pathway, and the larger the circle and the deeper the colour was, the more significant the pathway was. According to the screening conditions with impact >0, five metabolic pathways were obtained and considered to be closely related to liver injury. The pathway name and involved metabolite information were shown in Table 2 for details.

Effect of RG on the biomarkers of liver injury

The relative contents of biomarkers of liver injury in each group were shown in Figure 6. Compared with the MG group, the levels of lathosterol, oleic acid, bilirubin, linoleic acid, and palmitic acid in the RGG group significantly increased ($p < 0.05$), while the levels of cholic acid and chenodeoxycholic acid significantly decreased ($p < 0.05$). Combined with the result of metabolic pathway analysis, we found that the metabolic regulation of RG against liver injury was mainly related to steroid biosynthesis, linoleic acid metabolism, porphyrin and chlorophyll metabolism, and fatty acid biosynthesis.

Discussion

In this study, we found that the size, shape, and arrangement of hepatocytes in the liver tissue of the model group were abnormal, which indicated that the liver injury model we replicated was successful. After the preventive intervention of RG in different doses and positive control drugs, the damage of liver tissue recovered in different degrees, which showed that RG had a certain effect on liver injury.

In order to further evaluate the effect of Gentiana on liver injury, we measured some biochemical indexes such as ALT, AST, MDA, SOD, GSH, and GSH-PX, which can reflect the degree of liver damage. The levels of the above six indexes in the rats with liver injury were abnormal. After the preventive intervention of RG in different doses, the levels of each index recovered to the normal levels in various degrees and the therapeutic effect was similar to that of the positive control, indicating that RG had a good ability of scavenging free radicals and antioxidation.

It has been reported that some cytokines such as TNF-α, MCP-1, and IL-6 can directly or indirectly participate in the process of liver injury, induce or promote inflammatory response, and aggravate the degree of liver injury (Zhao et al. 2018; Xie et al. 2017; Qiao et al. 2017; Lu et al. 2017). Therefore, reducing the production of inflammatory factors can also alleviate liver injury to a certain extent. In this study, the levels of TNF-α, MCP-1, and IL-6 in the rats with liver injury were abnormal. After the preventive intervention of RG in different doses, the levels of each index recovered to the normal levels in various degrees and the therapeutic effect was similar to that of the positive control. The regulation of TNF-α and IL-6 was only significant in the high-dose group of RG. This showed that RG also had a good anti-inflammatory effect.

Through the analysis of biochemical indexes, we can know that the mechanism of RG against liver injury may be related to the elimination of free radicals and the enhancement of anti-oxidation and anti-inflammatory ability in liver tissue. In order to further study the metabolic mechanism of RG against liver injury, we selected the serum samples of the control group, model group, and medium-dose RG group for metabonomics study. In metabonomics study, eight potential biomarkers of liver injury were identified, and five metabolic pathways were found to be closely related to liver injury through the metabolic pathway analysis, among which the four metabolic pathways of steroid biosynthesis, linoleic acid metabolism, porphyrin and
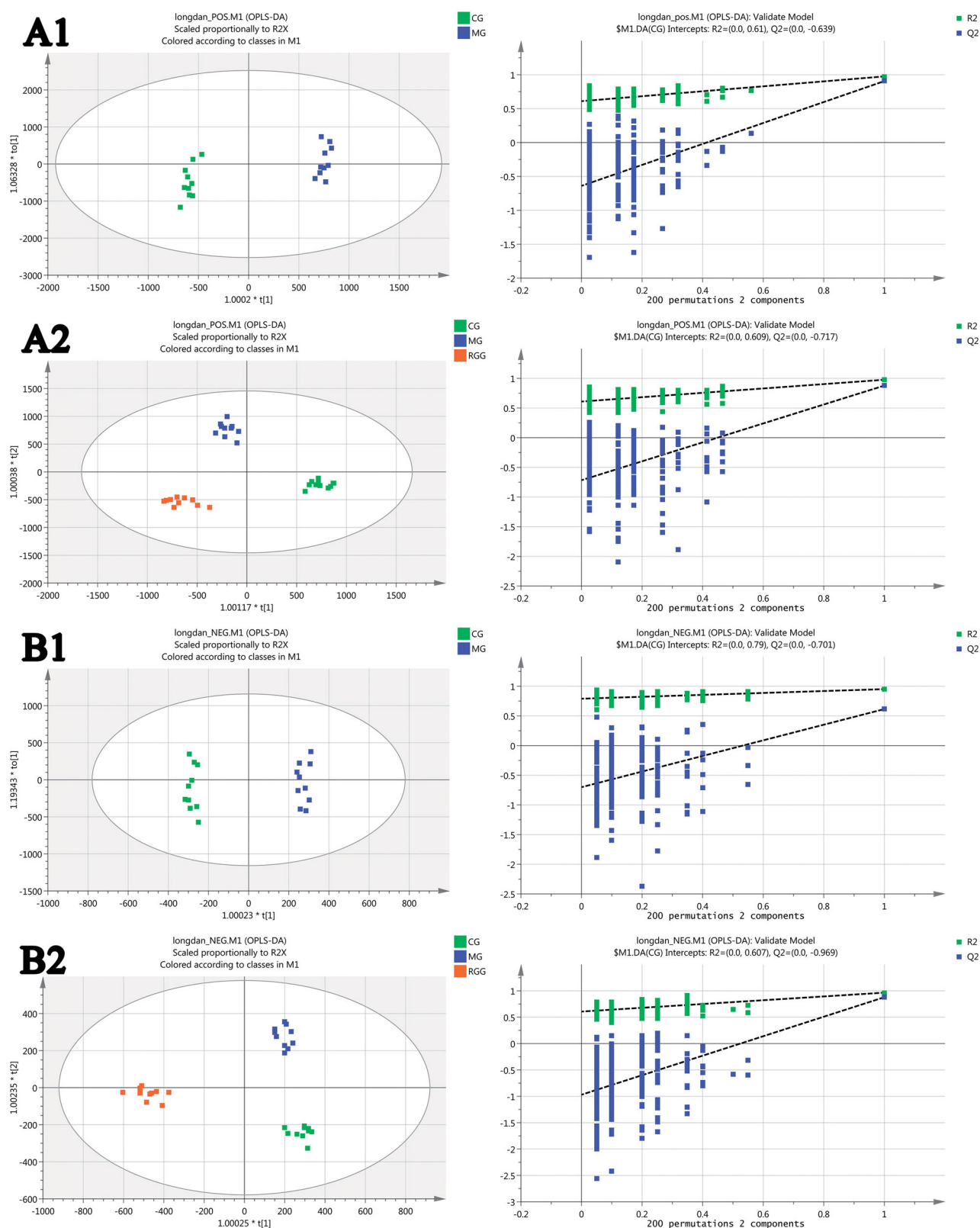
Figure 4. The scores of orthogonal partial least squares discriminant analysis and their 200 times permutation tests: (A1) CG vs. MG score under positive ion mode; (A2) All groups score under positive ion mode; (B1) CG vs. MG score under negative ion mode; (B2) All groups score under negative ion mode (model parameters-A1: $R^2Y = 0.794$, $Q^2 = 0.728$; A2: $R^2Y = 0.978$, $Q^2 = 0.876$; B1: $R^2Y = 0.994$, $Q^2 = 0.968$; B2: $R^2Y = 0.973$, $Q^2 = 0.894$).

chlorophyll metabolism, and fatty acid biosynthesis were significantly improved after the preventive intervention of RG.

The steroid is an essential hormone in the biological process of the body (Jeanneret et al. 2016), which plays an important role in regulating water and salt balance, protein, fat, metabolism, and stress response (Schiffer et al. 2019). Steroid biosynthesis is a multi-step process controlled by pituitary hormones, which drives the formation of specific tissue steroids through

Table 1. Potential biomarker information of liver injury.

HMDB ID	Compound name	RT/min	VIP	Formula	ms/ms	Error/ppm	Ion mode	MG ↑↓ vs. CG
0001170	Lathosterol	14.462	5.74	$C_{27}H_{46}O$	$428.38656[M + ACN + H]^+$; $410.37599[M + ACN + H − H_2O]^+$; $136.10994[M + ACN + H − H_2O − C_{20}H_{34}]^+$; $122.09429[M + ACN + H − H_2O − C_{20}H_{34} − CH_2]^+$	5	+	→
0000207	Oleic acid	13.554	5.67	$C_{18}H_{34}O_2$	$281.24787[M − H]^-$; $263.2373[M − H − H_2O]^-$; $111.11719[M − H − C_9H_{18} − CO_2]^-$; $97.06069[M − H − C_9H_{18} − CO_2 − CH_2]^-$	3	−	→
0000054	Bilirubin	7.549	4.55	$C_{33}H_{36}N_4O_6$	$619.28905 [M + Cl]^-$; $321.15731[M + Cl − C_{17}H_{18}N_2O_3]^-$; $335.17296[M + Cl − C_{16}H_{16}N_2O_3]^-$;	0	−	→
0000673	Linoleic acid	15.746	3.64	$C_{18}H_{32}O_2$	$325.23808[M + FA − H]^-$; $307.22751[M + FA − H − H_2O]^-$; $255.15983[M + FA − H − C_5H_{10}]^-$; $105.01898[M + FA − H − C_{16}H_{28}]^-$;	1	−	→
0000619	Cholic acid	4.309	3.61	$C_{24}H_{40}O_5$	$453.28552[M + FA − H]^-$; $435.27495[M + FA − H − H_2O]^-$; $389.26947[M + FA − H − H_2O − CH_2O_2]^-$	1	−	←
0001043	Arachidonic acid	15.265	3.37	$C_{20}H_{32}O_2$	$303.23221[M − H]^-$; $259.24237[M − H − CO_2]^-$; $149.09644[M − H − C_{10}H_{18}O]^-$	2	−	←
0000518	Chenodeoxycholic acid	4.663	3.01	$C_{24}H_{40}O_4$	$437.29046[M + FA − H]^-$; $419.27989[M + FA − H − H_2O]^-$; $401.26933[M + FA − H − 2H_2O]^-$; $393.30063[M + FA − H − CO_2]^-$;	1	−	←
0000220	Palmitic acid	12.305	2.63	$C_{16}H_{32}O_2$	$301.23803[M + FA − H]^-$; $283.22746[M + FA − H − H_2O]^-$; $159.06588[M + FA − H − C_{10}H_{22}]^-$; $131.03458[M + FA − H − C_{12}H_{26}]^-$	1	−	→

Note: "↑" represents the up-regulation; "↓" represents the down-regulation. 'FA' is an abbreviation for formic acid.
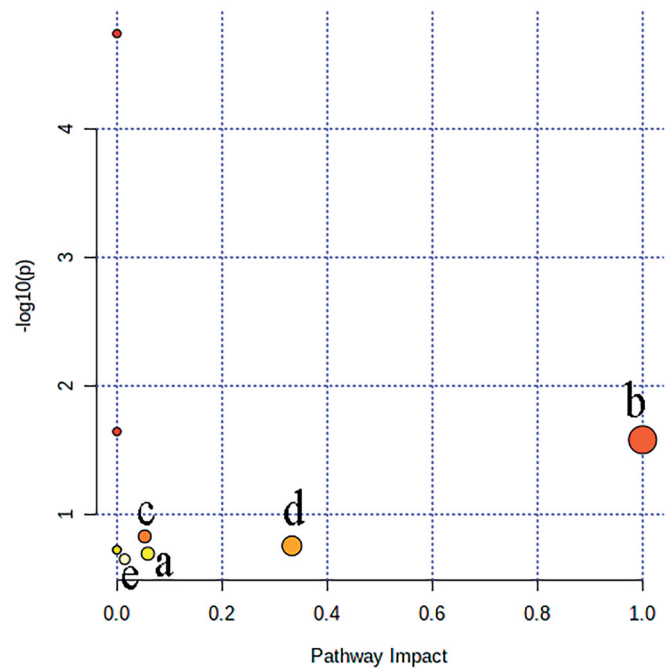

Figure 5. The result of metabolic pathway analysis of potential biomarkers of liver injury: (a) Steroid biosynthesis; (b) Linoleic acid metabolism; (c) Porphyrin and chlorophyll metabolism; (d) Arachidonic acid metabolism; (e) Fatty acid biosynthesis.

Table 2. Metabolic pathway information of impact > 0.

Pathway name	Impact	Total	Hits	Involved metabolite
Steroid biosynthesis	0.0588	42	1	Lathosterol
Linoleic acid metabolism	1.0	5	1	Linoleic acid
Porphyrin and chlorophyll metabolism	0.05288	30	1	Bilirubin
Arachidonic acid metabolism	0.33292	36	1	Arachidonic acid
Fatty acid biosynthesis	0.01472	47	1	Palmitic acid

cAMP signalling pathway (Issop et al. 2013). Steroidogenesis starts from the transport of substrate cholesterol from the cell to the mitochondrial inner membrane in the liver. Under the action of the steroidogenic enzyme CYP11A1, cholesterol is transformed into steroid hormone with biological activity (Rege et al. 2019). Lathosterol, a biomarker of liver injury found in this study, was an important molecule in the steroid biosynthesis pathway. Moolla et al. (2020) had used urinary steroid metabolome detection to perform the accurate non-invasive diagnosis and staging of non-alcoholic fatty liver disease, proving that the steroid biosynthesis pathway was closely related to liver function. In our study, rats treated with RG showed an increased level of lathosterol, indicating that RG can improve the steroid biosynthesis of rats with liver injury.

Linoleic acid is an essential fatty acid in human nutrition, and it is the basic material to form the cell membrane and enzyme of the organism (Spector and Kim 2015). It can enhance metabolism, regulate the endocrine system and promote lipid metabolism (Ebrahimi-Mameghani et al. 2016). Linoleic acid also acts as a catalyst for cholesterol metabolism and has the effect of reducing cholesterol and blood lipids in human blood (Pintus et al. 2013). A previous study found that the metabolic process of linoleic acid is mainly related to oxidative stress and inflammation. When the body is stimulated, linoleic acid is released from phospholipids and further generates inflammatory mediators (Khazen et al. 2007). The expression of linoleic acid, a biomarker of liver injury, was abnormal in this study, indicating
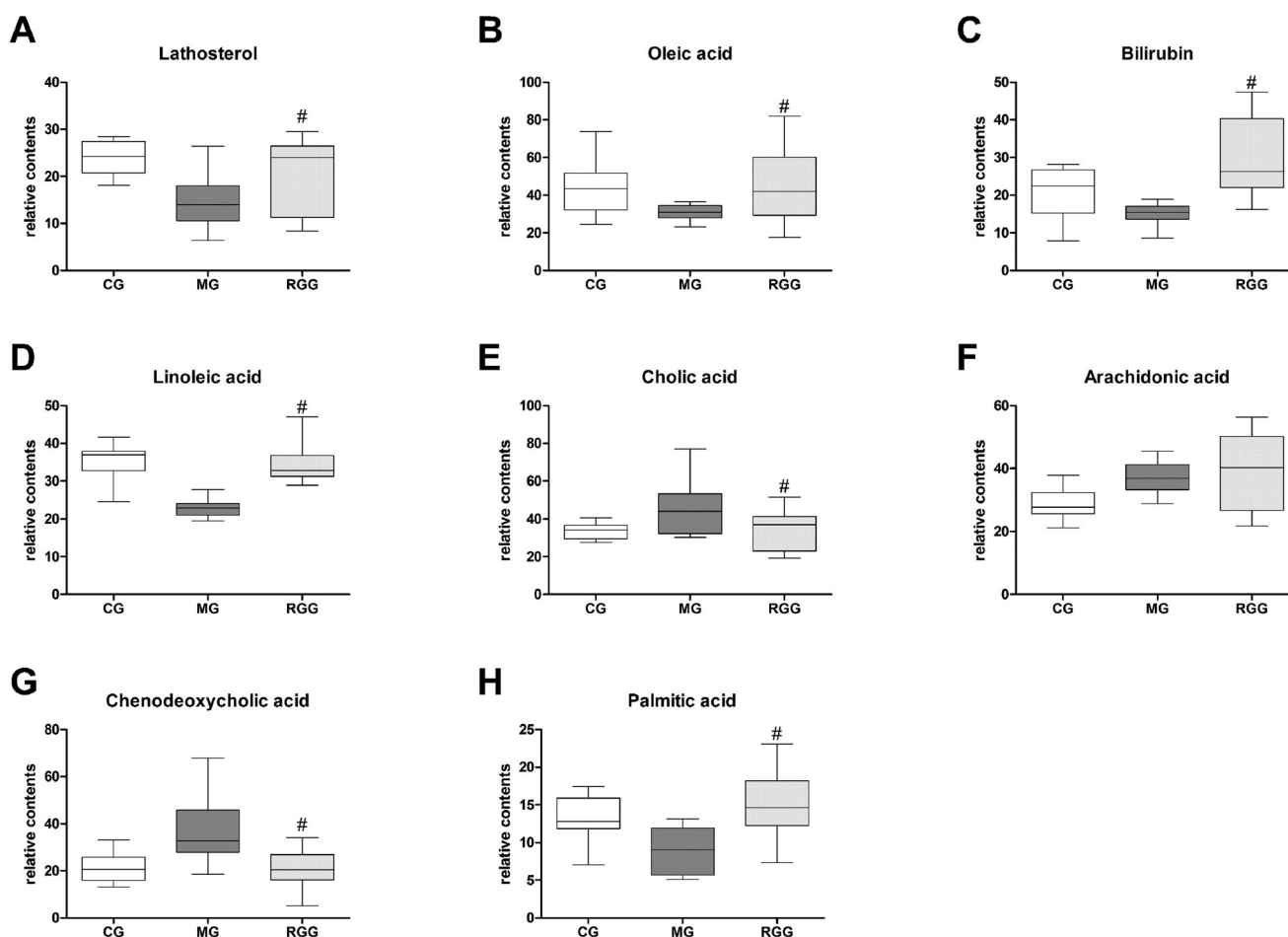
Figure 6. The relative content of biomarkers of liver injury of rats among diverse groups ($n = 10$): (A) Lathosterol level; (B) Oleic acid level; (C) Bilirubin level; (D) Linoleic acid level; (E) Cholic acid level; (F) Arachidonic acid level; (G) Chenodeoxycholic acid level; (H) Palmitic acid level. The relative content of metabolites was characterised by the peak area of each sample. [#]$p < 0.05$ when compared with the MG group.

that the metabolism of llinoleic acid was disordered and more inflammatory factors could be produced in the state of liver injury. Rats treated with RG showed increased levels of linoleic acid, indicating that RG can improve linoleic acid metabolism of rats with liver injury.

Bilirubin is an important molecule in the pathway of porphyrin and chlorophyll metabolism. Bilirubin is a kind of bile pigment, a yellow catabolic product of haem and a major metabolite of iron porphyrin *in vivo*. The role of bilirubin in the mechanism of liver injury is still controversial. Some studies revealed that bilirubin exhibited a high level when encountering liver injury (Li et al. 2021). However, bilirubin has the antioxidant and anti-inflammatory function at a physiological concentration (Ziberna et al. 2016), which is also an important indicator of assessing liver function in the clinic (Kusakabe et al. 2020). The abnormal expression of bilirubin in this study indicated that porphyrin and chlorophyll metabolism were in disorder in the state of liver injury. Rats treated with RG showed an increased level of bilirubin, indicating that RG can improve porphyrin and chlorophyll metabolism of rats with liver injury.

Fatty acids are the simplest kind of fat, and they are the components of many more complex fats. With sufficient oxygen supply, fatty acids can be oxidised and decomposed into carbon dioxide and water, releasing a lot of energy. Therefore, fatty acids are one of the main energy sources of the body (Karam et al. 2020). A large number of studies showed that fatty acids were closely related to liver injury (Han et al. 2018; Wang et al. 2015).

Palmitic acid, a biomarker of liver injury found in this study, is an important molecule in the pathway of fatty acid biosynthesis. The abnormal expression of palmitic acid in this study indicated that fatty acid biosynthesis was disordered in the state of liver injury. Rats treated with RG showed increased level of palmitic acid, indicating that RG can improve fatty acid biosynthesis of rats with liver injury.

To sum up, the improvement of steroid biosynthesis, linoleic acid metabolism, porphyrin and chlorophyll metabolism, and fatty acid biosynthesis may be the metabolic mechanism of RG protecting the liver. The results can help us understand the specific mechanism of RG against liver injury. However, there are some deficiencies in this study. The biomarkers of liver injury obtained in this study are still relatively limited and need further clinical verification. RG is rich in chemical components, including monoterpenes, polysaccharides, alkaloids, flavonoids, steroids, coumarins, volatile oils, and lactones (Lv et al. 2018). The results of this study provide some encouragement for our future research and development of new drugs against liver injury.

Conclusions

In this study, we found that the mechanism of RG protecting the liver may be related to the elimination of free radicals and the enhancement of antioxidation and anti-inflammatory ability in liver tissue. Eight potential biomarkers of liver injury were screened out by metabonomics analysis, and five significant

metabolic pathways were obtained. The metabolic pathways of steroid biosynthesis, linoleic acid metabolism, porphyrin and chlorophyll metabolism, and fatty acid biosynthesis were significantly improved after the intervention of RG, which may be the metabolic mechanism of RG against liver injury.

Disclosure statement

No potential conflict of interest was reported by the author(s).

Funding

References

Chen X, Cai W, Lin J, Yu H. 2018. Clinical observation of Xieqing pills combined with Shengjiang powder for insomnia and anxiety of syndrome of liver depression transforming into fire. J New Chin Med. 50:63–66.

Chinese Pharmacopoeia Commission. 2015. Pharmacopoeia of the people's Republic of China (Part I). Beijing: The Medicine Science and Technology Press of China.

Ding J. 2020. Effects of gentiopicroside on ANIT-induced cholestasis in rats. China Pharm. 23:2133–2137.

Ebrahimi-Mameghani M, Jamali H, Mahdavi R, Kakaei F, Abedi R, Kabir-Mamdooh B. 2016. Conjugated linoleic acid improves glycemic response, lipid profile, and oxidative stress in obese patients with non-alcoholic fatty liver disease: a randomized controlled clinical trial. Croat Med J. 57(4): 331–342.

Han H, Xu L, Xiong K, Zhang T, Wang Z. 2018. Exploration of hepatoprotective effect of gentiopicroside on alpha-naphthylisothiocyanate-induced cholestatic liver injury in rats by comprehensive proteomic and metabolomic signatures. Cell Physiol Biochem. 49(4):1304–1319.

Issop L, Rone MB, Papadopoulos V. 2013. Organelle plasticity and interactions in cholesterol transport and steroid biosynthesis. Mol Cell Endocrinol. 371(1–2):34–46.

Jeanneret F, Tonoli D, Rossier MF, Saugy M, Boccard J, Rudaz S. 2016. Evaluation of steroidomics by liquid chromatography hyphenated to mass spectrometry as a powerful analytical strategy for measuring human steroid perturbations. J Chromatogr A. 1430:97–112.

Karam J, Bibiloni M, Pons A, Tur JA. 2020. Total fat and fatty acid intakes and food sources in Mediterranean older adults requires education to improve health. Nutr Res. 73:67–74.

Khazen W, M'Bika JP, Collinet M, Tramoni M, Chany C, Achour A, Forest C. 2007. Differentiation-dependent expression of interferon gamma and toll-like receptor 9 in 3T3-F442A adipocytes. Biochimie. 89(5):669–675.

Kusakabe J, Hata K, Tanaka S, Omae K, Okamura Y, Tajima T, Tamaki I, Miyauchi H, Kubota T, Tanaka H, et al. 2020. Prognostic index consisting of early post-transplant variables <2 weeks in adult living-donor liver transplantation. Hepatol Res. 50:741–753.

Li M, Bai Z, Zhang C, Ma Z. 2021. Meta-analysis of fufang yiganling capsules against serum makers of anti-tuberculosis drug-induced liver injury. World Chin Med. 16:1977–1981.

Lu C, Lin X, Huang Q, Wei J. 2017. Protective effect and mechanism of methyl helicteres on chronic liver injury induced by CCl_4 in rats. Chin J Exp Tradit Med Form. 23:141–147.

Luan J, Ju D. 2018. Inflammasome: a double-edged sword in liver diseases. Front Immunol. 9:2201.

Lv X, Sun J, Xu S, Cai Q, Liu Y. 2018. Rapid characterization and identification of chemical constituents in Gentiana radix before and after wine-processed by UHPLC-LTQ-Orbitrap MS^n. Molecules. 23(12):3222.

Moolla A, de Boer J, Pavlov D, Amin A, Taylor A, Gilligan L, Hughes B, Ryan J, Barnes E, Hassan-Smith Z, et al. 2020. Accurate non-invasive diagnosis and staging of non-alcoholic fatty liver disease using the urinary steroid metabolome. Aliment Pharmacol Ther. 51(11):1188–1197.

Okubo S, Miyamoto M, Ito D, Takami K, Ashida K. 2016. Albumin and apo-lipoprotein H mRNAs in human plasma as potential clinical biomarkers of liver injury: analyses of plasma liver-specific mRNAs in patients with liver injury. Biomarkers. 21(4):353–362.

Pintus S, Murru E, Carta G, Cordeddu L, Batetta B, Accossu S, Pistis D, Uda S, Elena-Ghiani M, Mele M, et al. 2013. Sheep cheese naturally enriched in α-linolenic, conjugated linoleic and vaccenic acids improves the lipid profile and reduces anandamide in the plasma of hypercholesterolaemic subjects. Br J Nutr. 109(8):1453–1462.

Plumb RS, Johnson KA, Rainville P, Smith BW, Wilson ID, Castro-Perez JM, Nicholson JK. 2006. UPLC/MS(E); a new approach for generating molecular fragment information for biomarker structure elucidation. Rapid Commun Mass Spectrom. 20(13):1989–1994.

Qiao J, Zang Y, Miao Y, Cao L, Li Y, Miao M. 2017. Protective effects and mechanisms of ursolic acid on acute alcohol-induced liver injury in mice. Pharm Clin Chin Mater Med. 33:14–17.

Qu Z, Li F, Ma C, Liu J, Li S, Wang W. 2015. Effects of Gentiana scabra Bage on expression of hepatic type I, III collagen proteins in Paragonimus skrjabini rats with liver fibrosis. Asian Pac J Trop Med. 8(1):60–63.

Rege J, Turcu AF, Else T, Auchus RJ, Rainey WE. 2019. Steroid biomarkers in human adrenal disease. J Steroid Biochem Mol Biol. 190:273–280.

Ren L, Sun D, Zhou X, Yang Y, Huang X, Li Y, Wang C, Li Y. 2019. Chronic treatment with the modified Longdan Xiegan Tang attenuates olanzapine-induced fatty liver in rats by regulating hepatic de novo lipogenesis and fatty acid beta-oxidation-associated gene expression mediated by SREBP-1c, PPAR-alpha and AMPK-alpha. J Ethnopharmacol. 232: 176–187.

Schiffer L, Barnard L, Baranowski ES, Gilligan LC, Taylor AE, Arlt W, Shackleton CHL, Storbeck KH. 2019. Human steroid biosynthesis, metabolism and excretion are differentially reflected by serum and urine steroid metabolomes: a comprehensive review. J Steroid Biochem Mol Biol. 194: 105439.

Spector AA, Kim HY. 2015. Discovery of essential fatty acids. J Lipid Res. 56(1):11–21.

Wang X, Luo J, Chen R, Zha X, Pan L. 2015. Dendrobium huoshanense polysaccharide prevents ethanol-induced liver injury in mice by metabolomic analysis. Int J Biol Macromol. 78:354–362.

Wu G, Chen L, Gu Y, Hong Y, Ma J, Zheng N, Zhong J, Liu AJ, Sheng L, Zhang W, et al. 2020. Exploring the mechanism underlying the cardioprotective effect of shexiang baoxin pill on acute myocardial infarction rats by comprehensive metabolomics. J Ethnopharmacol. 259:113001.

Xia K, Jiang M, Cui B, Zhang Y, Zheng J, Wu Y, Nan J, Lian L. 2017. Protective effects of Gentiana manshurica Kitagawa on D-galactosamine/lipopolysaccharide-induced fulminant hepatic failure in mice. China J Tradit Chin Med Pharm. 32:3162–3166.

Xie Q, Huang X, Li J, Chen Z, Zhang S, Huang R. 2017. Protective effect of aqueous extract of Richeriella gracilis against liver injury in mice induced by carbon tetrachloride. J Guangxi Med Univ. 34:181–184.

Yang B, Yang Q, Zhang A, Wang X. 2019. Research progress of traditional Chinese medicine based on metabolomics technology. China Med Her. 16: 24–28.

Zeeshan M, Hamidi M, O'Keeffe T, Hanna K, Kulvatunyou N, Tang A, Joseph B. 2019. Pediatric liver injury: physical examination, fast and serum transaminases can serve as a guide. J Surg Res. 242:151–156.

Zhang B, Qi X, Cai Q. 2020. Metabolomic study of raw and bran-fried Atractylodis Rhizoma on rats with spleen deficiency. J Pharm Biomed Anal. 182:112927.

Zhang B, Sun J, Jiang Y, Ma S, Cai Q. 2019. Liver protecting effect of total polysaccharides and total iridoid glycosides from wine-processed Gentiana scabra Bge. Cent South Pharm. 17:1001–1005.

Zhao X, Li G, Hu Y, Yi R, Song J. 2018. Improvement effects and mechanism research of polyphenol extracts from Kudingcha on carbon tetrachloride induced hepatic damage in mice. Sci Technol Food Ind. 39:289–295.

Ziberna L, Martelanc M, Franko M, Passamonti S. 2016. Bilirubin is an endogenous antioxidant in human vascular endothelial cells. Sci Rep. 6: 29240.